Clim Dyn (2018) 51:4157–4168
DOI 10.1007/s00382-017-3646-5

Detecting hydrological consistency between soil moisture and precipitation and changes of soil moisture in summer over the Tibetan Plateau

X. Meng[1,6] · R. Li[2] · L. Luan[1,3] · S. Lyu[4,5] · T. Zhang[1] · Y. Ao[1] · B. Han[1] · L. Zhao[1] · Y. Ma[1,3]

Received: 28 June 2016 / Accepted: 16 March 2017 / Published online: 29 March 2017

Abstract As the first purely multi-decadal satellite-based soil moisture product that spans over 35 years (from November 1978 to December 2013) on a daily basis designed for climate application, the applicability of the European Space Agency (ESA) soil moisture product, including the hydrological consistency between the product and the observed precipitation and the product continuity on the Tibetan Plateau (TP) were investigated. The results show that there is significant degree between the ESA soil moisture product and the observed precipitation. The positive anomaly of the ESA soil moisture product can reflect the occurrences of precipitation, but the precipitation may not definitely lead to soil moisture anomaly, which largely depends on the precipitation amounts. For climate application, large number of missing gaps was shown on the west of the TP, where it is considered that the retrieval algorithms are largely affected by the permafrost covered in this region, leaving the ESA soil moisture product for further improvement. In application, the ESA soil moisture product was used to study the response of surface soil moisture to climate change on the TP. With the rapid warming and the overall wetting of the TP, soil moisture increases on the central of the TP with the increase of precipitation, and decreases in the southeast TP with the precipitation deduction. However, it decreases in the west TP, where it was probably influenced by both the insignificant precipitation changes and the significant increase of evaporation.

Keywords Hydrological consistency · ESA soil moisture product · Soil moisture · Precipitation · Trends · Tibetan Plateau

This paper is a contribution to the special issue on East Asian Climate under Global Warming: Understanding and Projection, consisting of papers from the East Asian Climate (EAC) community and the 13th EAC International Workshop in Beijing, China on 24-25 March 2016, and coordinated by Jianping Li, Huang-Hsiung Hsu, Wei-Chyung Wang, Kyung-Ja Ha, Tim Li, and Akio Kitoh.

✉ X. Meng
mxh@lzb.ac.cn

1 Key laboratory of Land Surface Process and Climate Change in Cold and Arid Regions, Northwest Institute of Eco-Environment and Resources, Chinese Academy of Science, Lanzhou 730000, China

2 Neimenggu Meteorological Center, Neimenggu 010051, China

3 University of Chinese Academy of Sciences, Beijing 100049, China

4 Plateau Atmosphere and Environment Key Laboratory of Sichuan Province, School of Atmospheric Sciences, Chengdu University of Information Technology, Chengdu 610225, China

5 Collaborative Innovation Center on Forecast and Evaluation of Meteorological Disasters, Nanjing, University of Information Science and Technology, Nanjing 210044, China

6 Zoige Plateau Wetlands Ecosystem Research Station, Northwest Institute of Eco-Environment and Resources, Chinese Academy of Science, 320 Donggang West Road, Lanzhou 730000, China

1 Introduction

The Tibetan Plateau (TP), which covers an area of approximately 2.5×10^6 km^2 and with more than half of the area over 4000 m above sea level, is the highest and largest highland in the world. With extensive glaciers and permafrosts, the TP is the source of many rivers in Asia, which is called as the "Asian Water Tower" (Cui et al. 2015; Duan et al. 2011; Yao et al. 2012; You et al. 2013b, 2016b). In addition, it has profound influences on not only the local climate but also the climate of the Asian continent, even on the global climate through its thermal and dynamic forcing (Duan et al. 2012, 2013; Ma et al. 2014b; Wu and Zhang 1998). It also strongly influences the environmental changes in China, Asia, and even the Northern Hemisphere (Guo and Wang 2013; Shen et al. 2015; Wu et al. 2012; Yang et al. 2011). With the global warming, climate and environmental changes of the TP and its substantial effects have attracted a rapidly growing number of interests (Cuo et al. 2013; Gao et al. 2014; Ma et al. 2014a; Song et al. 2011; Tian et al. 2014; Wu and Zhang 1998; You et al. 2013a).

With the global warming, the warming on the TP is more rapidly and larger than its surrounding regions and the warming rate of the TP is even 1.5 times of that of the global warming, showing that the TP is also an indicator and amplifier of the global warming (Kuang and Jiao 2016; Liu and Chen 2000; You et al. 2016a; Zhang et al. 2013). Under the rapid warming circumstances, most regions of the TP have been experiencing wetting in the last three decades (Yin et al. 2016). The accelerated climate change on the TP has caused many environmental changes, such as permafrost degradation, glacier retreat and snow melt etc. As a result, significant changes in hydrology and water resources occurred on the TP (Cuo et al. 2013; van der Velde et al. 2012; Yang et al. 2010, 2011; Yao et al. 2012).

As one of the important hydrological factors, soil moisture responses to climate change quickly and interacts with the overlaying atmosphere through surface energy and water balances, substantially leading to a feedback to regional climate (Betts 2009; Boe 2013; Findell and Eltahir 2003; Fischer et al. 2007; Huang and Margulis 2013; Lintner and Neelin 2009; Seneviratne et al. 2010; Siqueira et al. 2009; Wang et al. 2007). It is also a key variable in numerous environmental applications, including the hydrological modelling, weather and short-term climate forecasting (Zeng et al. 2015). In addition, changes of soil moisture on the TP can influence the sensible heating of the TP, resulting in formation and variations to Asian monsoon, influencing the climate change in Asian (Duan et al. 2011; Ma et al. 2009; Wu et al. 2012; Wu and Zhang 1998; Zhao and Kellogg 1988). Under future climate scenarios, the soil moisture deficits will increase in many places with higher evaporative demand driving and soil moisture may play an increasingly important role in climate change (Dirmeyer et al. 2013). Van der Velde et al (2014) found a wetting trend of soil moisture was shown by defined normalized soil moisture anomalies over the TP using the Special Sensor Microwave Imagers (SSM/I's) retrievals. However, due to the large uncertainties of models and observations over the TP, the complicated hydrology responses to climate warming led to different results when using different models and observations, especially on the different regions of the TP. For example, Gao et al. (2015b) quantifies the aridity changes on the TP, showing that stations located in the arid and semi-arid northwestern TP were becoming significantly wetter, and half of the stations in the semi-humid eastern TP were becoming drier, though not significantly, in the recent 3 decades. Gao et al. (2015a) also found that runoff decreased significantly in large part of the TP, while Su et al. (2016) showed that runoff increased due to the glacier melting and rainfall enhancement. It is important to understand how soil moisture on the TP response with the global warming using different observations.

Due to the special geographical environment and harsh climate conditions, an alternative way to get in-situ soil moisture observations is to obtain soil moisture from satellite microwave remote sensing (Zeng et al. 2015). Over the past several decades, researchers have exerted great efforts on the development of soil moisture retrieval algorithms and produced lots of soil moisture products, including the National Aeronautics and Space Administration (NASA) AMSR-E soil moisture product (Njoku and Chan 2006), the Land Parameter Retrieval Model (LPRM) soil moisture product (Owe et al. 2008), the Japan Aerospace Exploration Agency (JAXA) AMSR-E and AMSR2 soil moisture products (Koike et al. 2004), the SMOS soil moisture product (Kerr et al. 2012), the ASCAT soil moisture product (Naeimi et al. 2009) and the Essential Climate Variable (ESA) soil moisture product developed by the European Space Agency (ESA)(Dorigo et al. 2015; Liu et al. 2011, 2012; Wagner et al. 2012). Zeng et al. (2015) assessed the reliability of those seven soil moisture products using the in-situ measurements from three networks which represent different climatic and vegetation conditions on the TP, showing that almost all of the products can generally capture the soil moisture dynamics well, with the ESA soil moisture product being closest to the absolute values of soil moisture observations. However, for a short-term droughts detection, Yuan et al. (2015) found that the ESA soil moisture product can only detect less than 30% of short-term drought (month to seasonal) month at in situ station scale on the TP, showing that there are still uncertainties in the ESA soil moisture products when being applied in different studies.

As a result, three main purposes encourage us to use the ECV soil moisture product to investigate soil moisture change over the TP. Firstly, for the ECV soil moisture product, it is necessary to assess how well the dataset performed when being used on the TP for climate change related research, because most satellite data have missing values or large errors over the TP due to the influence of complex topography and specific land surface lying such as the permafrost. Secondly, although Van der Velde et al. (2014) have presented a wetting trend of soil moisture over the TP, it is still necessary to study the change of soil moisture change over the TP using other datasets, because different datasets have been illustrated to show different changes over the TP, such as the runoff trend discussed above. Thirdly, the ECV soil moisture product have been assessed to be the best product on the TP compared with other products, leaving us an expect to investigate soil moisture change responded with climate change more reasonably.

This paper is organized as follows. Firstly, a simple test was performed firstly to assess the hydrological consistency of the ESA soil moisture product to reflect the short-term response of soil moisture to precipitation. References to as McCabe et al. (2008), the surface soil moisture condition (wet or dry) should relate to precipitation (or lack thereof) in the hours preceding the ESA soil moisture product. Then a trend analysis of the ESA soil moisture in summer and its relation to air temperature and precipitation change on the TP will be analyzed, to explore the response of soil moisture to climate change on the TP. At last, discussion of the data using on the TP will be discussed for further improvements of the data. This is also a pioneering work to understand how soil moisture response and react to regional precipitation changes on the TP.

2 Data and methods

2.1 The ESA soil moisture product

The ESA soil moisture product is developed by merging different active and passive microwave products into a single multi-decadal soil moisture product, and then extended and improved to produce the latest version. One of the basic purposes for producing the product is to the work of the United Nations Framework Convention on Climate Change (UNFCCC) and the Intergovernmental Panel on Climate Change (IPCC) for climate applications. The ESA soil moisture products were supported under the ESA'S Water Cycle Multi-Mission Observation Strategy (WACMOS) project and soil moisture Climate Change Initiative (CCI) projects (Liu et al. 2012; Wagner et al. 2012). It spans from November 1978 to December 2013, covering over 35 years with spatial resolution of 0.25° and temporal resolution of 1 day. It is the first purely multi-decadal satellite-based soil moisture product that was designed for climate applications. The ESA soil moisture product homogenizes and merges the six microwave based products, including the Scanning Multichannel Microwave Radiometer (SMMR) onboard Nimbus-7, the Special Sensor Microwave Imager (SSM/I) of the Defense Meteorological Satellite Program, the Tropical Rainfall Measuring Mission Microwave Imager (TMI), the AMSR-E onboard the Aqua satellite, the WinSAT satellite, and the AMSR2 boarded on the GCOM-W1 satellite for the passive data sets, and the scatter meters (SCAT) onboard the European Remote Sensing satellites (ERS-1/2) and the ASCAT onboard the MetOp-A satellite for the active data sets (Liu et al. 2012). The latest version 2.0 product consists of the "active product", the "passive product", and the "combined product" blended based on the first two products. The time step centered at 0:00 UTC in the product. The "combined product" in summer (June, July and August) from 1979 to 2013 was used in this study. As this work is also an advanced assessment for the ESA soil moisture product in climate applications, we didn't fill in the gap because lots of values on the TP are missed; leaving references for the ESA soil moisture products updates.

2.2 The meteorological observations

The observational meteorological dataset used in this study includes the monthly climatology of air temperature and precipitation with a spatial resolution of 0.5° from 1979 to 2013, and the hourly precipitation datasets merged with the Automatic Weather Station (AWS) observations and the Climate Prediction Center Morphing Technique (CMORPH) in a spatial resolution of 0.1° in June in 2009. All the data are obtained from the Climatic Data Center, the National Meteorological Information Center, China Meteorological Administration (http://data.cma.cn/site/index.html), which is responsible for preserving, monitoring, assessing, and providing public access to the Nation's treasure of climate and historical weather data and information. The 0.5° monthly climatology was produced by interpolating observations of meteorological stations combining the Digital Elevation Model (DEM) by using the Thin Plate Spline method. The 0.1° hourly precipitation product was generated by merging the Automatic Weather Station (AWS) observations (more than 30,000 AWSs totally in China) and the Climate Prediction Center Morphing Technique (CMORPH). Bias of the 0.1° hourly precipitation product was controlled in 10%, while it is 20% in the heavy-rainfall and the sparsely observed regions, such as south China and the TP. The monthly climatology datasets of air temperature and precipitation are used to study the response of soil moisture to climate change, while the hourly precipitation data is used to evaluate the hydrological consistency of the soil moisture with the precipitation. As the TP is experiencing an overall wetting trend in recent years, and the ESA soil moisture can detect the long-term drought, here the hydrological consistency of soil moisture responses with precipitation was examined when the precipitation having positive anomaly. So, June 2009 is selected as an example for it is a typical positive month for precipitation from 2008 to 2015, since the hourly precipitation datasets only spans from 2008 until 2015.

2.3 Method for detecting the hydrological consistency between soil moisture and precipitation

The key point of assessing hydrologic consistency, is the inherent difficulty in validating remote sensing measurements; partly because the ground "validation" data represents different spatial scales and, often, different measurements (e.g. gravimetric soil moisture versus soil emissivity) (McCabe et al. 2008). In addition, the limited observational sites lead to large uncertainties of the spatial representativity, especially over the Tibetan Plateau, which is one of the most special and least explored areas on earth. As an evaluation of the ESA soil moisture product has been performed on the TP using the observational network Zeng et al. (2015), and the data can be used for a long-term drought detection in the work of Yuan et al. (2015), except for short-term drought (month to seasonal), here a simple approach for assessing hydrological consistency in McCabe et al. (2008) is used to assess the ability of the ESA soil moisture product's response to precipitation in the very short time scale (hourly to daily). The method is to assess if the surface soil moisture condition (wet or dry) relate to precipitation (or lack thereof) in the hours preceding the precipitation observation, and to what extent, changes in soil moisture can reflect the precipitation.

2.4 Method for trend analysis of soil moisture changes with climate warming

The Mann–Kendall test for a trend and a linear slope were used to detect and estimate trends in annual soil moisture series (Yue and Pilon 2004; Yue et al. 2002). The Mann–Kendall test is a nonparametric method without considering distribution of the observational data, and has been widely used to perform trend analysis in climate and hydrology research. A trend is considered to be statistically significant if it is significant at the 5% level. The formula is as follows (Yue and Pilon 2004; Yue et al. 2002):

The Mann–Kendall statistic P is calculated as:

$$S = \sum_{k=1}^{n-1} \sum_{j=k+1}^{n} sign\left(x_j - x_k\right) \dots sign\left(x_j - x_k\right) = \begin{cases} +1 & if\ \ x_j - x_k > 0 \\ 0 & if\ \ x_j - x_k = 0 \\ 1 & if\ \ x_j - x_k < 0 \end{cases} \tag{1}$$

The variance for the statistic S is defined by:

$$\mathrm{Var(S)} = \frac{n(n-1)(2n+5)}{18} \tag{2}$$

The test statistic Z is estimated as:

$$Z = \begin{cases} \frac{S-1}{\sqrt{\mathrm{VAR}(S)}} & if\ \ S > 0 \\ 0 & if\ \ S = 0 \\ \frac{S+1}{\sqrt{\mathrm{VAR}(S)}} & if\ \ S < 0 \end{cases} \tag{3}$$

In which Z follows a standard normal distribution, If $|Z| > Z_{1-\propto/2}$, where $\propto$ denotes the significant level, then the trend is significant.

3 Results

3.1 The hydrological consistency between soil moisture and precipitation

As was discussed in the work of McCabe et al. (2008), precipitation should lead to a positive anomaly for soil moisture i.e., the surface soil moisture condition (wet or dry) relate to precipitation (or lack thereof) in the hours preceding the precipitation observation and to some extent, changes in soil moisture can reflect the precipitation event as a positive anomaly. Referred to as McCabe et al. (2008), soil moisture anomaly was calculated based on the monthly average soil moisture in June 2009 on the TP. Figure 1 shows the selected positive soil moisture anomaly coupled with the precipitation events distributed throughout the month of the June in 2009. As was shown in Fig. 1, the soil moisture anomaly was on June 19, 25, 28, 29 and 30. Except for the missing values, there is a strong spatial consistency between the soil moisture anomaly and the precipitation map, i.e., when precipitation occurred, there is substantially precipitation positive anomaly lagged precipitation some hours (for example 6, 12 or 18 h). It was especially on June 25 and 28, in which distributions of soil moisture anomaly are quite similar with the precipitation pattern when it precedes the ESA overpass time 18 h. Similar results were shown in other days, except in a small area of the north TP on June 19, where the converse condition happened. Considering that the area of the converse case is very small, and there is still less precipitation occurred before the ESA soil moisture passing time, it is considered that there is a significant degree of spatial correlation between the ESA soil moisture and the precipitation overall.

Although a strong spatial coherence is shown in the patterns of the ESA soil moisture anomaly and the observed precipitation, it is necessary to quantify this agreement in advance. Figure 2 shows two separate experiments designed

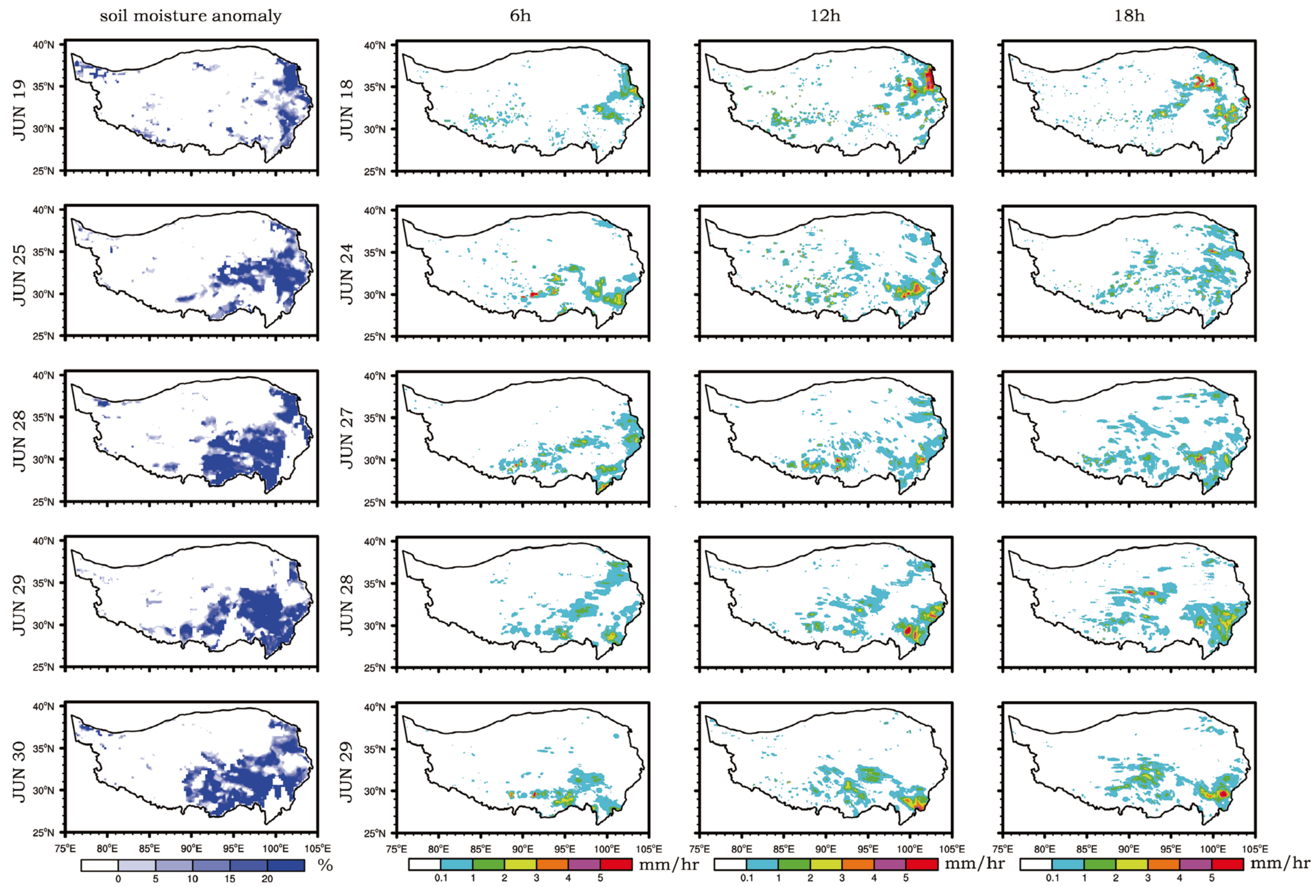

Fig. 1 Comparison of the ESA soil moisture anomaly for identified rain days during June 2009 over the TP. The observed hourly rainfall amounts (instantaneous rain-rate) are shown for 6, 12 and 18 h preceding the ESA overpass time (08 a.m. BT). Soil moisture anomaly is the difference between daily values and the monthly average, only showing a *positive* (wet) anomaly

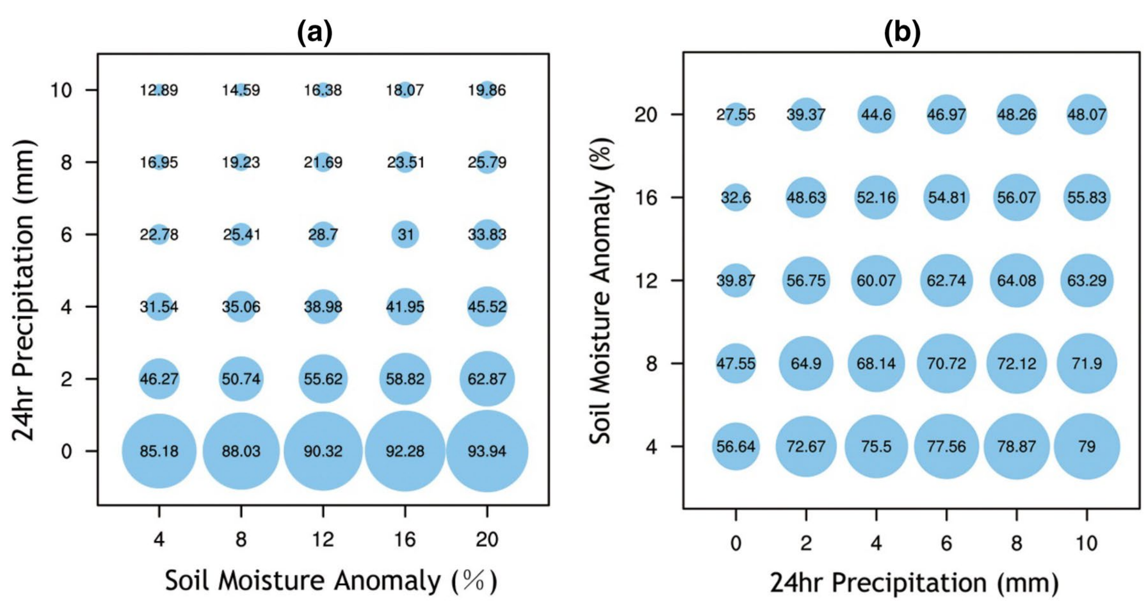

Fig. 2 Percentage of pixels satisfying the ESA soil moisture anomaly greater than some value x and having observed cumulative rainfall (24 h) greater than value y

to illustrate the level of agreement between the ECV soil moisture anomaly and the observed precipitation. Figure 2a shows the percentage of pixels (averaged over the 6 days in Fig. 1) that satisfy the ECV soil moisture anomalies greater than some value x, while also having observed cumulative precipitation (24 h total) greater than some value y; Fig. 2b shows the percentage of pixels that have observed cumulative precipitation (24 h total) greater than some value x, and also having an the ECV soil moisture anomaly greater than some value y. It can be seen that 85.18% of the pixels have a soil moisture anomaly greater than 4.0% and the observed precipitation in total greater than 0 mm. This indicates that when the soil is wet, there is good agreement that rain occurred. In addition, when the soil moisture anomaly is larger (for example it is 20%), more pixels (i.e., 93.94%) have rain occurred. However, if a statistic was made to show how many pixels with rain occurred and also with positive soil moisture happened in the substantial few hours, only 56.64% of pixels with 24-h cumulative precipitation greater than 0 mm showing a corresponding soil moisture anomaly greater than 4% (in Fig. 2b). This indicates that relative heavy rain events are better represented by the positive soil moisture. These results suggest that there is coupling between the ESA soil moisture and the observed precipitation. However, differences of strength of the soil moisture-coupling show that soil moisture positive anomaly is probably caused by precipitation, while precipitation may not sufficiently lead to soil moisture anomaly, which largely depends on the precipitation amounts or other influences such as the evapotranspiration.

3.2 Climatology and trend of soil moisture and precipitation on the TP

As most satellite products including the microwave and the optical remote sensing have missing values on the TP due to the topographic influences, the gaps were not filled when the number of missing years is greater than 10 (for the time series is from 1979 to 2013, 35 years totally), leaving them for references for further improvements and updates of the ESA products. Otherwise, the gaps of missing values are filled by linear interpolation. Figure 3 shows climatology and trend of the ESA soil moisture and precipitation from 1979 to 2013. As is shown in Fig. 3a, large area of the west TP has missing values in the ESA soil moisture product. In Fig. 3a, b, both soil moisture and precipitation show the similar pattern with two variables decrease from the southeast to the northwest of the TP, with the minimum in the desert in the north of the TP and the maximum in the southeast of the TP. However, the maximum of soil moisture is

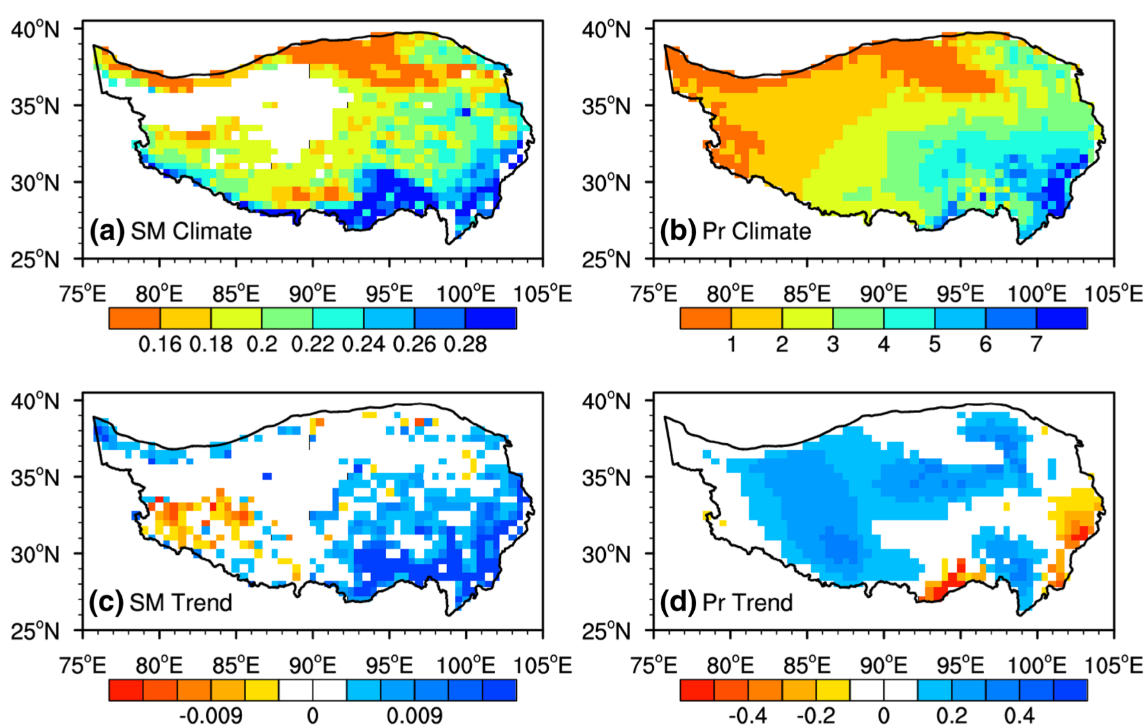

Fig. 3 Climatology and trend of soil moisture and precipitation in summer from 1979 to 2013. **a** Climatology of soil moisture; **b** climatology of precipitation; **c** trend of soil moisture; **d** trend of precipitation. In (**a**) and (**b**) the *white* regions represent pixels with missing values. In (**c**) and (**d**) the *white* regions represent pixels with missing values or pixels with trends not satisfying the statistical significance test or pixels with trends less than 0.003 m^3 m^{-3}/10 year for soil moisture and 0.1 mm/day.10year for precipitation.

in the valley of the south of the TP and also in the Hengduan Mountains in the southeast of the TP, while the maximum of precipitation is in the Hengduan Mountains. As the algorithm and the accuracy of the microwave retrieved soil moisture was largely influenced by vegetation, topography, etc., it is not surprised that climatology of soil moisture and precipitation differed in the south and the Hengduan Mountains where the impacts of valleys, mountains, and vegetation are large. Figure 3c shows that soil moisture increases in the southeast part of the TP, except for a small area in the west edge of TP from 1979 to 2013. In the southwest of the TP, soil moisture shows slightly decreasing trend. Precipitation enhances in most of the TP, particularly in the central and west of the TP, while it decreases in the valley of the south TP and the Hengduan Mountains. From Fig. 3c, d, it can be seen that only in a small region of the central TP and in the Hengduan Moutain, both soil moisture and precipitation increased significantly. In the northwest of the TP, soil moisture and precipitation shows inconsistent trends, with precipitation enhancement significantly while soil moisture changes did not passing the significant test. This result again indicates that the precipitation increased may not definitely result in soil moisture enhancement; some other factors may play important roles in different regions.

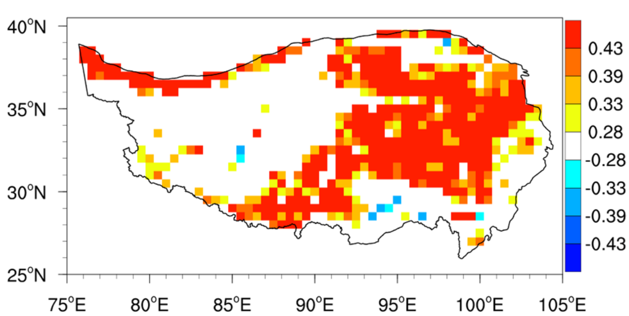

Fig. 4 Correlations between soil moisture and precipitation (only the correlations statistical significance at or above 95% level are shown)

Figure 4 shows correlations between the soil moisture and the precipitation with only the correlations statistical significance at or above 95% level were shown. In the central part of the TP, the ESA soil moisture coupled with precipitation well, with the correlation coefficient ranging from 0.33 to 0.43. In other regions, especially in the west, south and southeast of the TP, correlation between precipitation and soil moisture is weak. This is partly consistent with the hydrological consistency shown in Figs. 1 and 2. In the hydrological consistency detecting, it was shown that an increase of soil moisture was caused by precipitation enhancement, while the precipitation increases may not definitely result in soil moisture enhancement. So, it is partly considered that in the west of the TP, the response of soil moisture to precipitation is relatively weaker because the rainfall amount is relatively smaller and the soil is drier than that in other regions of the TP. Furthermore, with the climate warming, evapotranspiration increases over the most part of the TP (Yang et al. 2011; Yin et al. 2013), which may be another factor that results in the soil moisture reduce over the west of the TP.

Figure 5 shows annual changes of soil moisture anomaly and precipitation anomaly averaged on the TP. Correlation between the two changes is 0.53, showing that there is a relatively high correlation between soil moisture anomaly and precipitation anomaly. Variance of soil moisture is relatively weaker than precipitation. Instead, trend of soil moisture is relatively greater than that of precipitation. Positive soil moisture anomaly corresponds with positive precipitation anomaly better than the negative responses, for example, negative precipitation anomaly recovers from 1998, while soil moisture keeps in a low state until 2004. This further illustrates that soil moisture does not definitely

Fig. 5 Annual changes of soil moisture anomaly and precipitation anomaly averaged on the TP

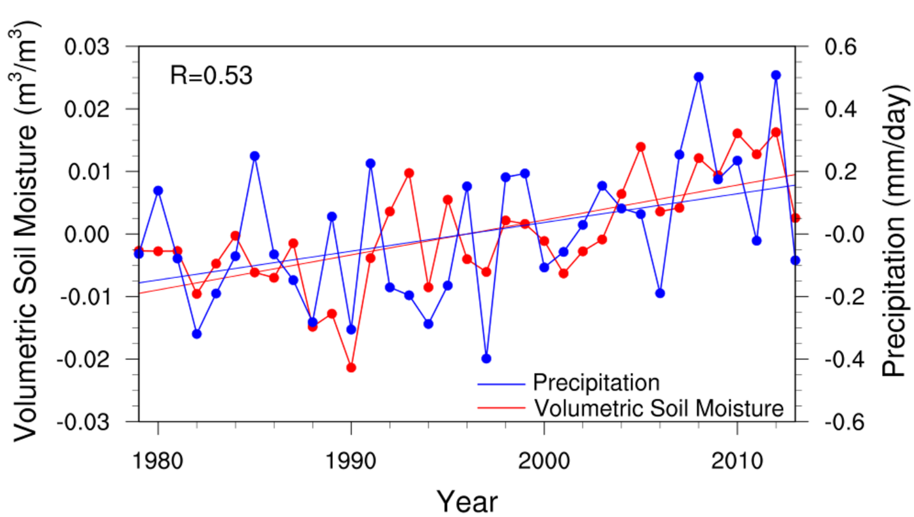

increase with precipitation enhancement due to the influences of other hydrological factors.

Figure 6 shows the Mann Kendall test and linear slope of soil moisture and precipitation time series. For the period from 1979 to 2013, the increasing trends of both soil moisture and precipitation are significant when averaging on the TP. From 1979 to 2003 for soil moisture and 1979 to 2002 for precipitation, neither variable increased significantly. The trend of soil moisture is 0.0001 $m^3\ m^{-3}\ 10a^{-1}$. From 2003 for soil moisture and 2002 for precipitation (which are mutation years in the Mann Kendall tests), both variables increase, with the significance and trend of soil moisture greater than those of precipitation. From 2003 to 2013, the trend of soil moisture is 0.0012 $m^3\ m^{-3}\ 10a^{-1}$, which is more rapidly than it increases from 1979 to 2003.

3.3 Responses of soil moisture to climate warming on the TP

Studies suggested that global warming have accelerated the hydrological cycle, especially on the TP (Held and Soden 2006; Yang et al. 2011; Yin et al. 2013, 2016; You et al. 2016b).

An analysis of seasonal variation in the water budget components demonstrated that the dominant water cycling arises from the processes of precipitation and evaporation that are typical in the eastern TP (Zhang et al. 2003). Observed and simulated evaporation show overall increasing trends, leading to decreased discharge on major TP water resource areas (semi-humid and humid zones in the eastern and southern TP) (Yin et al. 2013, 2016). Figure 7 shows partial correlations between trended and detrended soil moisture, precipitation and air temperature. It indicates that trend of soil moisture is significantly correlated with precipitation changes on the main central part of the TP (Fig. 7c). However, in the west and north of the TP where soil moisture shows slightly decreasing trend in the whole period (Fig. 7d), negative coupling between soil moisture and air temperature indicates that there is probability that the decrease of soil moisture in this region was caused by co-influence of the increase of evaporation and the slight changes of precipitation. To further investigate the probable influence of evaporation on the soil moisture, evaporation was calculated using the Advection-Aridity Model (AA Model) (Brutsaert and Stricker 1979) with site observations. Figure 8 shows the trend of evaporation in summer from 1979 to 2013 (only showing the sites with the change significance $p < 0.05$). It shows that the largest increase of evaporation was in the west TP with an enhancement of 1 ~ 1.5 mm per year. Evaporation increases in the north part secondly. Although the observation sites are limited, it can partly reflect the trend of the evaporation. So, slight decreases of soil moisture in the west and north parts of the TP may be caused by the rapid evaporation in these regions. As a result, both precipitation and air temperature play important role in the soil moisture changes on the TP. And the responses of soil moisture to climate change are regionally different.

4 Discussion

Considerable spatial coherence and hydrological consistency between the ESA soil moisture and the observed precipitation was observed in the previous analysis to explore the degree of the ESA soil moisture reflecting the occurred precipitation in a daily to monthly short-term scale. However, these detections do not focus on the converse condition how the ESA soil moisture responses when there is no precipitation. This is very important for drought or decreasing trend detection for soil moisture time series. As a result, it is more confidently to consider that the enhancement of soil moisture from 1979 to 2013 in the central part of the TP, where precipitation increases more significantly. This

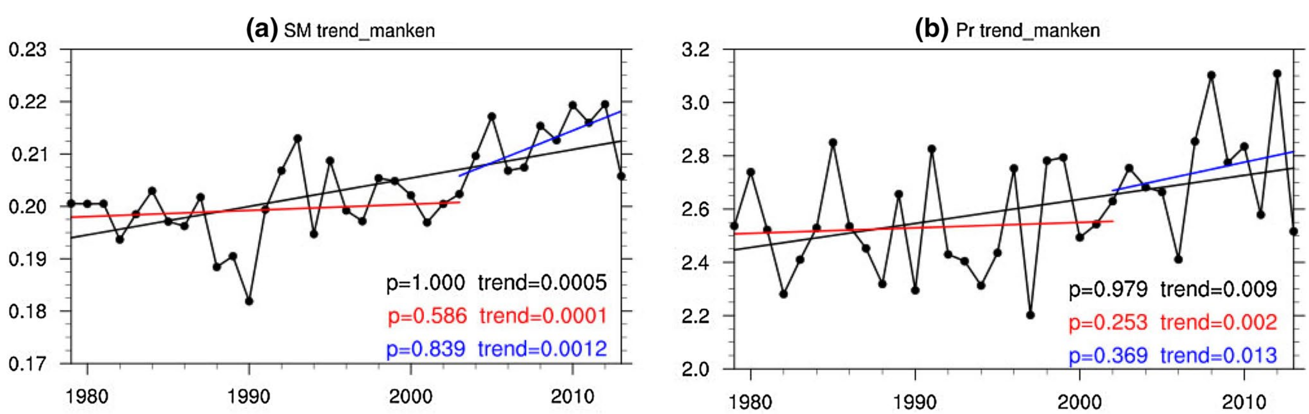

Fig. 6 Mann Kendall test and linear slope of soil moisture and precipitation time series. **a** Trend of soil moisture; **b** trend of precipitation

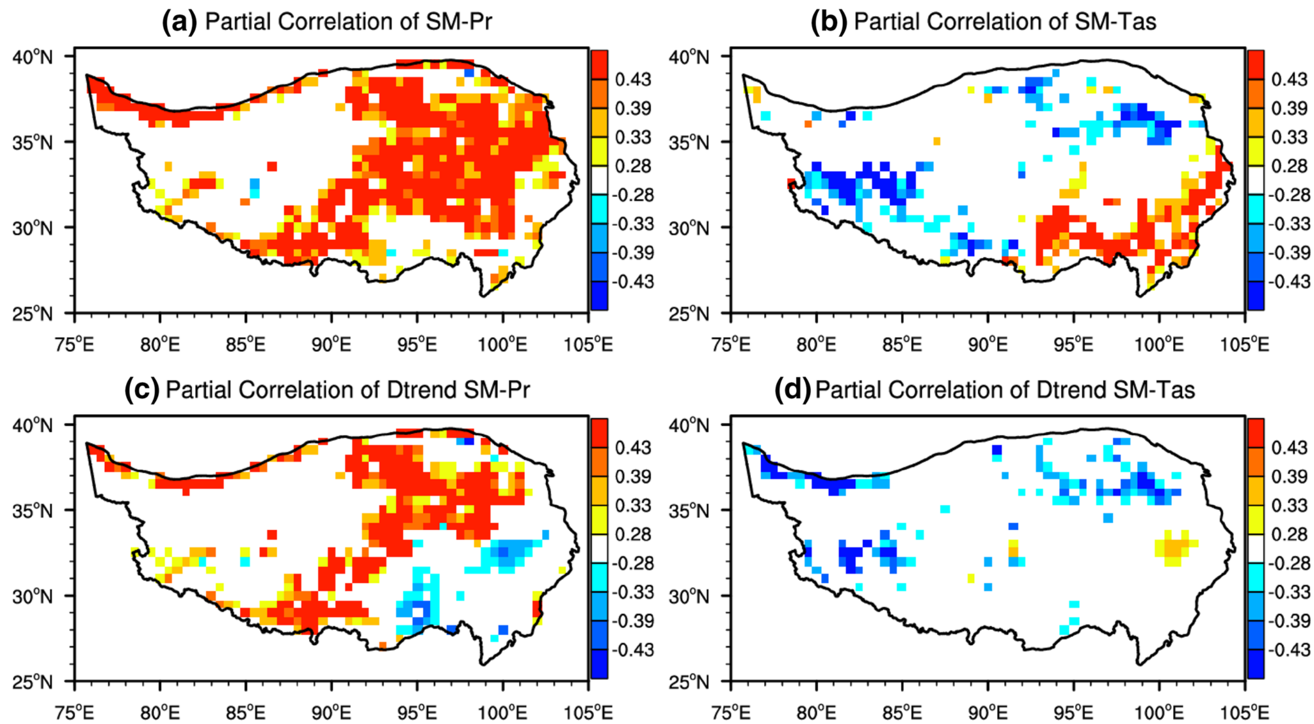

Fig. 7 Partial correlations between trended and detrended soil moisture, precipitation and air temperature. **a** Partial correlation between soil moisture and precipitation; **b** partial correlation between soil moisture and air temperature; **c** partial correlation of detrended soil moisture and precipitation; **d** partial correlation of detrended soil moisture and air temperature

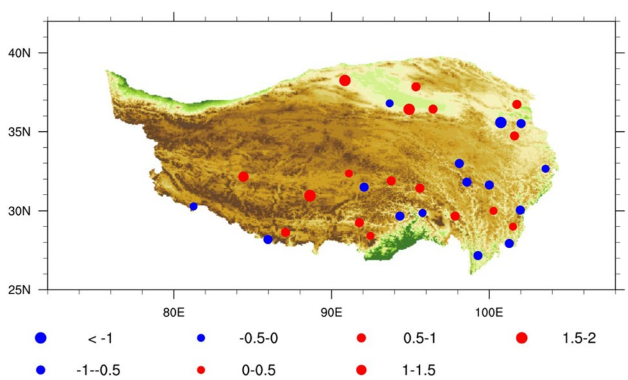

Fig. 8 Spatial distribution of trend of evaporation for the period 1979–2013 (mm/year) (with the significance $p<0.05$, *blue* indicates the negative trend, *red* indicates the positive trend)

result is consistent with the conclusion in the work of van der Velde et al. (2012). However, in the west TP where the ESA soil moisture decreases, there remain considerable uncertainties because the number of observational stations here are very few and the increase trend of precipitation is not significantly when the evaporation increases definitely.

On the south and southeast of the TP, where the ESA soil moisture increases but precipitation decreases in Fig. 1c, d, we would like to expect that there is uncertainty in the ESA soil moisture product. There are four reasons that can be considered. First, the observed stations in these two regions are relatively denser than that in the west of the TP. So, it is more confident to have a conclusion that precipitation in these two regions decreases in the whole time period. Secondly, evaporation over these areas has been illustrated to be increasing with the warming of the TP, leading to a decreasing factor for soil moisture changes. Thirdly, Runoff in these two regions has been found to be decreased severely (Gao et al. 2015a), which indirectly reflects the hydrological condition of these two regions. At last, landscapes of these two regions are forest and more densely vegetated area, and the topography are very complex, which are two important factors that influence the retrieval of microwave remote sensing for soil moisture.

Crucial for climate applications is stable product continuity over time. To address the ESA soil moisture's ability to capture long-term trends, Dorigo et al. (2012) assessed trends in the ESA soil moisture product for the period of 1988 to 2010 by comparing with products from GLDAS-Noah and ERA-Interim land surface models, lending confidence in the dataset's capability for climate application.

Furthermore, Loew et al. (2013) pointed out that even though the ESA soil moisture has a large potential for climate trend assessments, discontinuities in the time series due to changing input observation systems should be

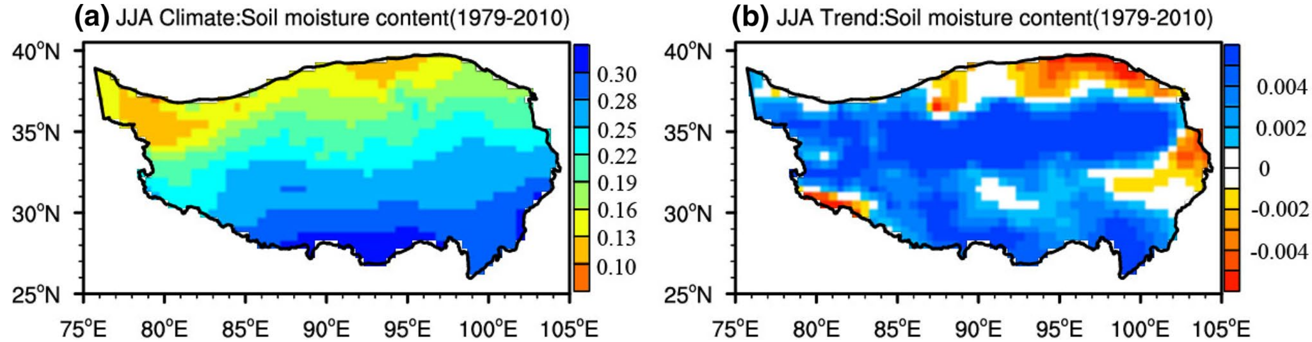

Fig. 9 Climatology and trend of soil moisture in summer from 1979 to 2010 based on GLDAS Noah data. **a** Monthly averaged climatology of soil moisture; **b** trend of soil moisture from 1979 to 2010

carefully accounted for. As the ESA soil moisture is applied for climate application on the TP, it is obvious that large number of gaps in the datasets as was shown in Fig. 1a, leaving space for product further improvements. Figure 9 shows climatology and trend of soil moisture in summer from 1979 to 2010 based on GLDAS Noah dataset on the TP. It can be seen that the GLDAS soil moisture shows similar spatial distribution with precipitation and the ESA soil moisture product. The difference is that climatology of the soil moisture and precipitation decreases from southeast to northwest gradually while the GLDAS soil moisture reduces from the south to the west of the TP. In addition, soil moisture increases significantly in most part of the TP, except that in the desert region on the north TP and the northeast of Western Sichuan Plateau. In the central of the TP, the ESA product shows a consistent trend with the GLDAS product.

5 Conclusion

Owing to the terrain complexity, high elevation, scarce observations and multiple landscapes such as glaciers, permafrost etc., most satellite remote sensing retrievals have missing values on the TP. In this work, the consistency between the ESA soil moisture product and the observed precipitation was examined to assess the ability of the ESA dataset in exploring the short-term (daily to monthly) changes of soil moisture, particularly for the changes with precipitation positive anomaly. The results show that there is significant correlation between the ESA soil moisture product and the observed precipitation. The positive anomaly of the ESA soil moisture product can well reflect the occurrences of precipitation, but precipitation may not definitely lead to soil moisture anomaly, which largely depends on the precipitation amounts.

As the first purely multi-decadal satellite-based soil moisture product that spans over 35 years on a daily basis designed for climate application, large number of missing gaps can be found on the west of the TP. In this region, about 10-year (35 years totally) data were missing, resulting in discontinuities for the climate application. As the influence by cloud for microwave remote sensing retrievals could be neglected, it is considered that landscapes affect the retrieve algorithm. Almost the entire region is covered by permafrost, which can directly influence the retrieval of soil moisture. Furthermore, observational stations in this region are sparse, which partly prevents the algorithm development in advance. All these left a broad space for both microwave soil moisture retrieval algorithm development and enhanced observations requirement on the TP in the next future.

With the rapid warming and overall wetting of the TP, soil moisture in the central of the TP shows increasing trend, with the west showing a decreasing trend. Trends of soil moisture are consistent with the changes of precipitation in the main central of the TP. However, in the northeast of the Western Sichuan Plateau, the ESA soil moisture shows negatively trend with precipitation, which was partly considered to be caused by the retrieval bias in these topographic and vegetarian areas. In addition, there are many uncertainties in the hydrological responses to climate warming in these regions, such as the responses of runoff, glacier melting (Gao et al. 2015a; Su et al. 2016), which may be other reasons for the negative correlation between soil moisture and precipitation over here. Totally, soil moisture increases with the increase of precipitation, and decreases with the precipitation decrease, except in the west TP, where it was probably influenced by both the insignificant precipitation changes and the significant increase of evaporation.

Acknowledgements This study was under the auspices of the Chinese National Science Foundation Programs (91437102; 41375015, 91537214 and 41675157), the CAEERI STS Funding (Y651671001), the Chinese Academy of Youth Innovation and Promotion, CAS (2014384) and the China Special Fund for Meteorological Research in the Public Interest (GYHY201506001-04). We thank the European Space Agency (ESA) and the China Meteorological Administration (CAM) for providing the soil moisture product and the observational datasets.

References

Betts AK (2009) Land-surface-atmosphere coupling in observations and models. J Adv Model Earth Sy 1:691–695. doi:10.3894/james.2009.1.4

Boe J (2013) Modulation of soil moisture-precipitation interactions over France by large scale circulation. Clim Dyn 40:875–892. doi:10.1007/s00382-012-1380-6

Brutsaert W, Stricker H (1979) An advection-aridity approach to estimate actual regional evapotranspiration. Water Resour Res 15(2):443–450. doi:10.1029/WR015i002p00443

Cui Y, Duan A, Liu Y, Wu G (2015) Interannual variability of the spring atmospheric heat source over the Tibetan Plateau forced by the North Atlantic SSTA. Clim Dyn 45:1617–1634. doi:10.1007/s00382-014-2417-9

Cuo L, Zhang Y, Wang Q, Zhang L, Zhou B, Hao Z, Su F (2013) Climate change on the northern Tibetan Plateau during 1957–2009: spatial patterns and possible mechanisms. J Clim 26:85–109. doi:10.1175/jcli-d-11-00738.1

Dirmeyer PA, Jin Y, Singh B, Yan XQ (2013) Trends in land-atmosphere interactions from CMIP5 simulations. J Hydrometeorol 4:829–849. doi:10.1175/jhm-d-12-0107.1

Dorigo W, de Jeu R, Chung D, Parinussa R, Liu Y, Wagner W, Fernández-Prieto D (2012) Evaluating global trends (1988–2010) in harmonized multi-satellite surface soil moisture. Geophys Res Lett 39:L18405. doi:10.1029/2012GL052988

Dorigo WA et al (2015) Evaluation of the ESA CCI soil moisture product using ground-based observations. Remote Sens Env 162:380–395. doi:10.1016/j.rse.2014.07.023

Duan A, Li F, Wang M, Wu G (2011) Persistent weakening trend in the spring sensible heat source over the Tibetan Plateau and its impact on the Asian summer monsoon. J Clim 24:5671–5682. doi:10.1175/jcli-d-11-00052.1

Duan A, Wu G, Liu Y, Ma Y, Zhao P (2012) Weather and climate effects of the Tibetan Plateau. Adv Atmos Sci 29:978–992. doi:10.1007/s00376-012-1220-y

Duan A, Hu J, Xiao Z (2013) The Tibetan Plateau summer monsoon in the CMIP5 simulations. J Clim 26:7747–7766. doi:10.1175/jcli-d-12-00685.1

Findell KL, Eltahir EAB (2003) Atmospheric controls on soil moisture-boundary layer interactions. Part I: framework development. J Hydrometeorol 4:552–569. doi:10.1175/1525-7541

Fischer EM, Seneviratne SI, Vidale PL, Lüthi D, Schär C (2007) Soil moisture-atmosphere interactions during the 2003 European summer heat wave. J Clim 20:5081–5099. doi:10.1175/JCLI4288.1

Gao Y, Cuo L, Zhang Y (2014) Changes in moisture flux over the Tibetan Plateau during 1979–2011 and possible mechanisms. J Clim 27:1876–1893. doi:10.1175/jcli-d-13-00321.1

Gao Y, Leung LR, Zhang Y, Cuo L (2015a) Changes in moisture flux over the Tibetan Plateau during 1979–2011: insights from a high-resolution simulation. J Clim 28:4185–4197. doi:10.1175/JCLI-D-14-00581.1

Gao Y, Li X, Leung LR, Chen D, Xu J (2015b) Aridity changes in the Tibetan Plateau in a warming climate. Environ Res Lett 10:34013–34024. doi:10.1088/1748-9326/10/3/034013

Guo D, Wang H (2013) Simulation of permafrost and seasonally frozen ground conditions on the Tibetan Plateau, 1981–2010. J Geophys Res 118:5216–5230. doi:10.1002/jgrd.50457

Held IM, Soden BJ (2006) Robust responses of the hydrological cycle to global warming. J Clim 19:5686–5699. doi:10.1175/jcli3990.1

Huang H-Y, Margulis SA (2013) Impact of soil moisture heterogeneity length scale and gradients on daytime coupled land-cloudy boundary layer interactions. Hydrol Process 27:1988–2003. doi:10.1002/hyp.9351

Kerr YH, Waldteufel P, Richaume P, Wigneron JP (2012) The SMOS soil moisture retrieval algorithm. IEEE T Geosci Remote 50:1384–1403. doi:10.1109/TGRS.2012.2184548

Koike T, Nakamura Y, Kaihotsu I, Davaa G, Matsuura N, Tamagawa K, Fujii H (2004) Development of an advanced microwave scanning radiometer (AMSR-E) algrithm for soil moisture and vegetation water content. Proc Hydaulic Eng 48:217–222. doi:10.2208/prohe.48.217

Kuang X, Jiao JJ (2016) Review on climate change on the Tibetan Plateau during the last half century. J Geophy Res Atmos 121:3979–4007. doi:10.1002/2015JD024728

Lintner BR, Neelin JD (2009) Soil moisture impacts on convective margins. J Hydrometeorol 10:1026–1039. doi:10.1175/2009JHM1094.1

Liu X, Chen B (2000) Climatic warming in the Tibetan Plateau during recent decades. Int J Climatol 20:1729–1742. doi:10.1002/1097-0088

Liu YY Dorigo WA, Parinussa RM, Jeu RAMD, Wagner W (2012) Trend-preserving blending of passive and active microwave soil moisture retrievals. Remote Sens Environ 123:280–297. doi:10.1016/j.rse.2012.03.014

Liu YY Parinussa RM, Dorigo WA, De Jeu RAM, Wagner W, van Dijk AIJM, McCabe MF, Evans JP (2011) Developing an improved soil moisture dataset by blending passive and active microwave satellite-based retrievals. Hydrol Earth Syst Sci 15:425–436. doi:10.5194/hess-15-425-2011

Loew A, Stacke T, Dorigo W, de Jeu R, Hagemann S (2013) Potential and limitations of multidecadal satellite soil moisture observations for selected climate model evaluation studies. Hydrol Earth Syst Sci 17:3523–3542. doi:10.5194/hess-17-3523-2013

Ma Y, Wang Y, Wu R, Hu Z, Yang K, Li M, Ma W, Zhong L, Sun F, Chen X, Zhu Z, Wang S, Ishikawa H (2009) Recent advances on the study of atmosphere-land interaction observations on the Tibetan Plateau. Hydrol Earth Syst Sci 13:1103–1111. doi:10.5194/hess-13-1103-2009

Ma Y, Han C, Zhong L, Wang B, Zhu Z, Wang Y, Zhang L, Meng C, Xu C, Amatya PM (2014a) Using MODIS and AVHRR data to determine regional surface heating field and heat flux distributions over the heterogeneous landscape of the Tibetan Plateau. Theor Appl Climatol 117:643–652. doi:10.1007/s00704-013-1035-5

Ma Y, Hu Z, Tian L, Duan A Yang K, Yang Y (2014b) Study progresses of the Tibet Plateau climate system change and mechanism of its impact on East Asia. Adv. Earth Sci 29:207–215

McCabe MF, Wood EF, Wójcik R, Pan M, Sheffield J, Gao H, Su H (2008) Hydrological consistency using multi-sensor remote sensing data for water and energy cycle studies. Remote Sens Environ 112:430–444

Naeimi V, Scipal K, Bartalis Z, Hasenauer S, Wagner W (2009) An improved soil moisture retrieval slgorithm for ERS and METOP

scatterometer observations. IEEE T Geosci Remote 47:1999–2013 doi:10.1109/TGRS.2008.2011617
Njoku EG, Chan SK (2006) Vegetation and surface roughness effects on AMSR-E land observations. IEEE T Geosci Remote 100:190–199. doi:10.1016/j.rse.2005.10.017
Owe M, de Jeu R, Holmes T (2008) Multisensor historical climatology of satellite-derived global land surface moisture. J Geophys Res 113:196–199. doi:10.1029/2007JF000769
Seneviratne SI Corti T, Davin EL, Hirschi MH, Jaeger EB, Lehener I, Orlowsky B, Teuling AJ (2010) Investigating soil moisture–climate interactions in a changing climate: a review. Earth Sci Rev 99:125–161. doi:10.1016/j.earscirev.2010.02.004
Shen M, Piao S, Jeong SJ, Zhou L, Zeng Z, Ciais P, Chen D, Huang M, Jin CS, Li LZ, Li Y, Myneni RB, Yang K, Zhang G, Zhang Y, Yao T (2015) Evaporative cooling over the Tibetan Plateau induced by vegetation growth. P Natl Acad Sci USA 112:9299–9304. doi:10.1073/pnas.1504418112
Siqueira M, Katul G, Porporato A (2009) Soil moisture feedbacks on convection triggers: the role of soil–plant hydrodynamics. J Hydrometeorol 10:96–112. doi:10.1175/2008JHM1027.1
Song M, Ma Y, Zhang Y, Li M, Ma W, Sun F (2011) Analyses of characteristics and trend of air temperature variation along the Brahmaputra Valley. Clim Environ Res 16:760–766
Su F, Zhang L, Ou T, Chen D, Yao T, Tong K, Qi Y (2016) Hydrological response to future climate changes for the major upstream river basins in the Tibetan Plateau. Global Planet Change 136:82–95
Tian L, Zhang Y, Zhu J (2014) Decreased surface albedo driven by denser vegetation on the Tibetan Plateau. Environ Res Lett 9:104001. doi:10.1088/1748-9326/9/10/104001
van der Velde R, Su Z, van Oevelen P, Wen J, Ma Y, Salama MS (2012) Soil moisture mapping over the central part of the Tibetan Plateau using a series of ASAR WS images. Remote Sens Env 120:175–187. doi:10.1016/j.rse.2011.05.029
van der Velde R, Salama MS, Pellarin T, Ofwono M, Ma Y, Su Z (2014) Long term soil moisture mapping over the Tibetan Plateau using special sensor microwave/imager. Hydrol Earth Syst Sci 18:1323–1337
Wagner W, Dorigo W, Jeu Rd, Fernandez D, Benveniste J, Haas E, Ertl M (2012) Fusion of active and passive microwave observations to create an Essential Climate Variable data record on soil moisture ISPRS Annals of the Photogrammetry, Remote Sensing and Spatial Information Sciences (ISPRS Annals) Volume I–7, XXII ISPRS Congress, Melbourne, Australia, 25 August–1 September 2012, 315–321
Wang G, Kim Y, Wang D (2007) Quantifying the strength of soil moisture-precipitation coupling and its sensitivity to changes in surface water budget. J Hydrometeorol 8:551–570. doi:10.1175/JHM573.1
Wu G, Zhang Y (1998) Tibetan Plateau forcing and the timing of the monsoon onset over South Asia and the South China sea. Mon Weather Rev 126:913–927. doi:10.1175/1520-0493
Wu G, Liu Y, Dong B, Liang X, Duan A, Bao Q, Yu J (2012) Revisiting Asian monsoon formation and change associated with Tibetan Plateau forcing: I. Formation. Clim Dyn 39:1169–1181. doi:10.1007/s00382-012-1334-z
Yang M, Nelson FE, Shiklomanov NI, Guo D, Wan G (2010) Permafrost degradation and its environmental effects on the Tibetan Plateau: a review of recent research. Earth Sci Rev 103:31–44. doi:10.1016/j.earscirev.2010.07.002
Yang K, Ye B, Zhou D, Wu B, Foken T, Qin J, Zhou Z (2011) Response of hydrological cycle to recent climate changes in the Tibetan Plateau. Clim Change 109:517–534. doi:10.1007/s10584-011-0099-4
Yao T, Thompson L, Yang W, Yu W, Gao Y, Guo X, Yang X, Duan K, Zhao H, Xu B, Pu J, Lu A, Xiang Y, Kattel DB, Joswiak D (2012) Different glacier status with atmospheric circulations in Tibetan Plateau and surroundings. Nature Clim Change 2:663–667. doi:10.1038/nclimate1580
Yin Y, Wu S, Zhao D (2013) Past and future spatiotemporal changes in evapotranspiration and effective moisture on the Tibetan Plateau. J Geophys Res 118:2013JD019609. doi:10.1002/jgrd.50858
Yin J, Zhan X, Zheng Y, Hain C R, Ek M, Wen J, Li F, Liu J (2016) Improving Noah land surface model performance using near real time surface albedo and green vegetation fraction. Agr Forest Meteorol 218–219:171–183. doi:10.1016/j.agrformet.2015.12.001
You Q, Fraedrich K, Min J, Kang S, Zhu X, Pepin N, Zhang L (2013a) Observed surface wind speed in the Tibetan Plateau since 1980 and its physical causes. Int J Climatol 34:1873–1882. doi:10.1002/joc.3807
You Q, Fraedrich K, Ren G, Pepin N, Kang S (2013b) Variability of temperature in the Tibetan Plateau based on homogenized surface stations and reanalysis data. Int J Climatol 33:1337–1347. doi:10.1002/joc.3512
You Q, Min J, Jiao Y, Sillanpää M, Kang S (2016a) Observed trend of diurnal temperature range in the Tibetan Plateau in recent decades. Int J Climatol 36:2633–2643. doi:10.1002/joc.4517
You Q, Min J, Kang S (2016b) Rapid warming in the Tibetan Plateau from observations and CMIP5 models in recent decades. Int J Climatol 36:2660–2670. doi:10.1002/joc.4520
Yuan X, Ma Z, Pan M, Shi C (2015) Microwave remote sensing of short-term droughts during crop growing seasons. Geophys Rez Lett 42:4394–4401. doi:10.1002/2015GL064125
Yue S, Pilon P (2004) A comparison of the power of the t test, Mann-Kendall and bootstrap tests for trend detection. Hydrol Sci J 49:21–37. doi:10.1623/hysj.49.1.21.53996
Yue S, Pilon P, Cavadias G (2002) Power of the Mann–Kendall and Spearman's rho tests for detecting monotonic trends in hydrological series. J Hydrol 259:254–271. doi:10.1016/S0022-1694
Zeng J, Li Z, Chen Q, Bi H, Qiu J, Zou P (2015) Evaluation of remotely sensed and reanalysis soil moisture products over the Tibetan Plateau using in-situ observations. Remote Sens Env 163:91–110. doi:10.1016/j.rse.2015.03.008
Zhang Y, Ohata T, Kadota T (2003) Land-surface hydrological processes in the permafrost region of the eastern Tibetan Plateau. J Hydrol 283:41–56. doi:10.1016/S0022-1694(03)00240-3
Zhang D, Huang J, Guan X, Chen B, Zhang L (2013) Long-term trends of precipitable water and precipitation over the Tibetan Plateau derived from satellite and surface measurements. J Quant Spectrosc Radiat Transfer 122:64–71. doi:10.1016/j.jqsrt.2012.11.028
Zhao Z-C, Kellogg WW (1988) Sensitivity of soil moisture to doubling of carbon dioxide in climate model experiments. Part II: the Asian monsoon region. J Clim 1:367–378. doi:10.1175/1520-0442